INFLUENCES OF THE SUCTION NOZZLE ON THE CHARACTERISTICS OF A PERIPHERAL PUMP AND AN EFFECTIVE METHOD OF THEIR REMOVAL

Senoo, Yasutoshi
Research Institute for Applied Mechanics, Kyushu University

https://doi.org/10.5109/7157946

出版情報：Reports of Research Institute for Applied Mechanics. 3 (11), pp.129-145, 1954-08. 九州大学応用力学研究所
バージョン：
権利関係：

Reports of Research Institute for Applied Mechanics
Vol. III, No. 11 August, 1954

INFLUENCES OF THE SUCTION NOZZLE ON THE CHARACTERISTICS OF A PERIPHERAL PUMP AND AN EFFECTIVE METHOD OF THEIR REMOVAL

By Yasutoshi SENOO

In the other paper[1] the present writer suggested that the characteristics of a peripheral pump might be improved if the influences of the suction nozzle could be removed. In this paper the development of the study in the line, both theoretical and experimental, are reported together with some results which verify the above mentioned idea.

In the first place the cause of the influences of the suction nozzle is studied: by proving that the influences of the immature development of the velocity profile are not important and that the turbulence is not yet sufficiently developed in the pumping passage near the nozzle, it is clarified that the latter is the source of those influences. In order to cancel these effects, the position of the entry of the pumping passage should be moved down-stream. By doing so, the fluid is disturbed by the impeller and the turbulence is thus fully developed, and then the turbulent fluid enters the pumping passage.

The suction nozzle of a pump is reformed into three kinds of forms and their characteristics are compared with each other. It is shown that a pump modified in a suitable manner have much better characteristics than those of an old type.

1. Introduction. In the foregoing paper the present writer suggested that the characteristics of a pump might be remarkably influenced by the form of the entry of the pumping passage. As is shown in Figure 1, pressure gradient along the pumping passage near the suction nozzle is not so steep as that experienced at a point elsewhere. This tendency grows remarkable as the discharge is increased, and at last the local pressure in the pumping passage becomes lower than the suction pressure. In this region of low pressure cavitation can occur easily thus bringing about the fall of efficiency for

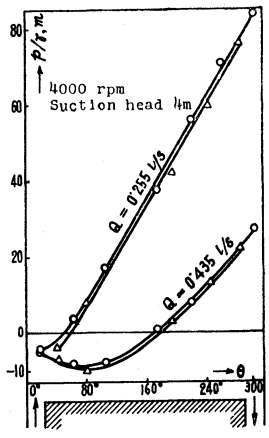

FIG. 1.
Pressure distribution along the pumping passage of an ordinary pump.

[1] Y. Senoo: Researches on peripheral pump. Reports of Research Institute for Applied Mechanics. Vol. III, No. 10.

a high suction height. The pressure distribution in the figure shows also that the effective length of the pumping passage is shorter than the structural length.

According to the theory already reported, in many cases it appears that the influence of the suction nozzle is chiefly responsible for the efficiency of an actual pump which is always lower than the value expected under the ideal condition. Accordingly, if the influence of the suction nozzle can be removed, the characteristics of a peripheral pump will be improved considerably.

2. The cause of the influence of the suction nozzle. In order to know whether and, if so, how the influence of the suction nozzle can be removed, it is necessary to know the cause and the mechanism. According to the opinion of the writer the influence can be attributed to two facts. The one is that the velocity profile across the pumping passage near the entry is very different from that prevailing downstream. The entry-effect of this kind can be found also in many pipe-flows and can be hardly removed. The other originates from the particular nature of the turbulence of the liquid near the entry. That is, being induced by the impeller the turbulence in the pumping passage is quite different in character from the usual turbulence of an ordinary pipe-flow, the former being much more intense than the latter. If the turbulence is induced by the impeller but is not yet sufficiently developed near the entry, the states of flow and of pressure gradient must be very different from each of them in the other region where the turburence is fully developed.

In the next section the influence of the entry will be calculated theoretically assuming that the flow is fully turbulent right from the entry. The result shows that if this assumption be correct the influenced zone would be very short. This is incompatible with the experimental result, therefore the assumption used above is proved incorrect. Accordingly, we can summarize as follows: the cause of the influence of the entry is due to the fact that the turdulence is not yet fully developed in the pumping passage near the entry. If the suction port is properly modified and the turbulence induced by the impeller can be fully developed at the entry, the influence of the entry will be removed and the characteristics of a pump will be necessarily improved.

3. Calculation of the influence of the entry. In order to clarify the nature of the influence of the entry, a calculation is performed assuming that the liquid near the entry is as fully turbulent just as in the remaining passage. Because the turbulence is induced by the impeller, it has the following character: the intensity of the turbulence varies as the peripheral velocity of the impeller, while the mixture length increases in proportion to the distance from the fixed wall and further the turbulent viscosity at the fixed wall must coincide with the molecular viscosity of the liquid. All of these were verified in the paper already published.

Since the purpose of this calculation is only to decide whether the assumption is correct or not, a rough estimation of the influence of the entry under the assumed condition will be sufficient for the present purpose. An expression of the velocity distribution in the pumping passage is assumed in a form containing four variables, each of which is estimated from the equations of motion and the several boundary conditions as a function of the distance from the entry and of the discharge. The equations are solved and the pressure distribution along the pumping passage is determined. The detail of the calculation will be shown in the appendix of this paper. The result shows that the influence of the entry under the assumed condition is not remarkable at all. Accordingly, we can arrive at the conclusion: the influence of the entry is not due to the immature development of the velocity profile but to that of the turbulence of the liquid near the entry.

4. The mechanism of the turbulence. As was already reported, the mechanism of the turbulence induced in the pumping passage is visualized by the following picture, namely a number of lumps of the fluid filling the spaces between the vanes of the impeller are projected into the fluid in the pumping passage transmitting the momentum of the impeller to the fluid in the pumping passage. Because the impeller splashes the lumps of the fluid tangentially, the fluid cannot fill up the cross-sections at the suction nozzle and at the entry of the pumping passage; the position where the cross-section of the pumping passage is filled with the fluid which were thrusted away from the impeller is found far downstream from the suction nozzle. At the entry of the pumping passage, therefore, the intensity of the turbulence is not so strong as when fully developed. The experiment shows that the pressure gradient is small near the entry and becomes larger as the distance from the entry increases and at last attains to a final value. This experimental fact together with the result of the preceding calculation verify that the mechanism of the turbulence is just as was above mentioned.

The cross-sectional area is narrowed suddenly at the entry and here the fluid is accelerated. In the case of a peripheral pump of ordinary type the entry is not sufficiently far from the patition, so the fluid is not yet fully accelerated by the impeller. Accordingly, the fluid must be accelerated by the pressure difference between the suction port and the pumping passage, namely the pressure at the entry must be lower than the suction pressure. When the discharge pressure is high and the quantity of discharge is little, however, the mean velocity is small and in some cases the fluid flows even backward against the motion of the impeller in some part of the cross-section. In these cases the cross-section near the partition is filled completely with the fluid which has been accelerated by the impeller, and the influence of the entry is not remarkable and the influenced length is not long.

5. Reformation of the entry. The cause of the undesirable behavior of the flow at the entry was thus clarified, so we may easily remove it by

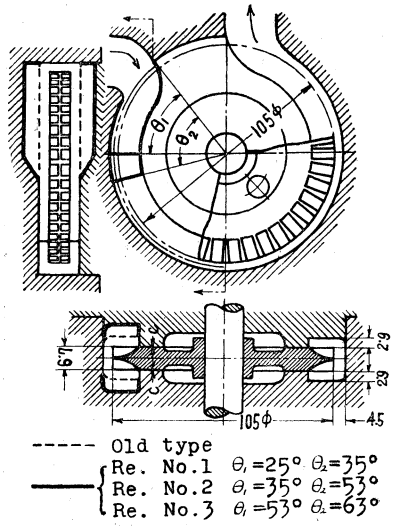

FIG. 2.

Structural reformations of the entry of the pumping passage.

a reformation of the entry. The entry has to be moved away from the patition and to be set at the position where the fluid is fully accelerated by the impeller.

In order to find the optimum position experimentally, the pump-characteristics are compared among the pumps with the entry of old type and with three kinds of the reformed entries. The detail of the reformation is shown in Figure 2. In each of these pumps the cross sectional area of the pumping passage is 117 mm^2 and that of the enlarged passage near the entry is 238 mm^2. As this figure shows, the pumping passage is connected with the suction nozzle with a spread of 25° even in the case of the old type. In the case of the Reformed No. 1 type, both sides of the pumping passage is scraped and the cross-sectional area is 238 mm^2 at the range $\theta = 0°$ to $\theta = 25°$. The area becomes gradually smaller as the angle θ increases and it becomes equal to that of the pumping passage at $\theta = 36°$. In the case of the Reformed No. 2 type, the passage is enlarged at the range $\theta = 0°$ to 36° and it gradually decreases its area to be connected with the pumping passage smoothly at $\theta = 53°$. In the case of the Reformed No. 3 type, the passage is enlarged at the range $\theta = 0°$ to 46° and it gradually decreases its area to be connected with the pumping passage smoothly at $\theta = 63°$.

The magnitude of the clearance for the internal leakage c was adjusted to be 0.05 mm for the old type, the Reformed No. 2 and No. 3 type pumps. However, since the impeller and the casing contacted each other and wore, the clearance increased to about 0.30 mm. The characteristics of the Reformed No. 1 type pump was measured at this increased clearance. The influence of the increase of the clearance was estimated theoretically and was verified experimentally using the data of the Reformed No. 2 type pump which were measured at both 0.05 mm and 0.30 mm clearance. Accordingly the performance of the Reformed No. 1 type pump with 0.05 mm clearance is rather accurately estimated from the experimental data of the pump with 0.30 mm clearance.

6. The pressure distribution in the pumping passage. In order to check whether the pressure decrease at the entry of the reformed type pumps is smaller than that at the old one, the best way is to measure the pressure distribution along the pumping passages and to compare them directly with each other.

Figure 3 shows the pressure distributions in the pumping passage of

these pumps, where ○ and △ are the measured values at the tip and the root of the vanes of the impeller respectively. Since there is secondary flow or turbulence in the pumping passage, the pressures measured through these small holes may be different from the true statical pressures there, but anyway they will not be far from the true values.

As the figure shows, in the case of the old type the pressure decrease at the entry is more remarkable than those of the reformed type pumps in spite of the lesser discharge. In the Reformed No. 1 type pump, since the cross-sectional area of the pumping passage is enlarged at the entry for a spread of 25° ($\theta = 0°$ to 25°), the pressure decrease at this range is slight and the pressure decreases again at the range $\theta = 30°$ to 60°.

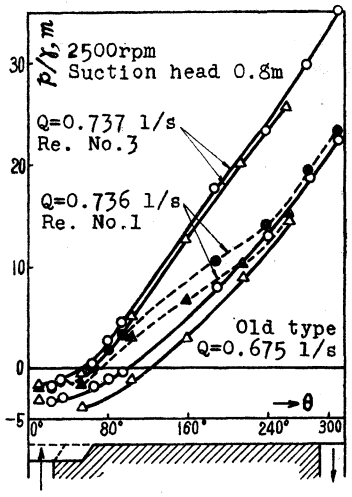

FIG. 3.
Effect of the reformation on the pressure distribution along the pumping passage.

In the case of the old type the cross-section seems to be large enough at the range $\theta = 0°$ to 25°, because the pumping passage is connected with the suction nozzle there. Neverthless the pressure at that point is quite lower than the suction pressure. In this case since neither side of the pumping passage is enlarged at all, the velocity of the iquid in both sides of the pumping passage at the suction nozzle will be nearly equal to that in both sides of the remaining pumping passage. Accordingly when the liquid flows into both sides of the passage from the suction nozzle, the liquid will be accelerated by the pressure difference, that is, the pressure at that point will be lower than the suction pressure. This fact shows that the depth of the pumping passage near the entry should be larger than that of the rest of the pumping passage, not only radially but also axially.

In the case of Reformed No. 3 type, since the pumping passage is enlarged so as to exclude the pressure decrease at any part of the pumping passage, the pressure increases monotonously along the pumping passage.

The pressure distribution curves of Reformed No. 1 type in Figure 3 show that the pressure gradient near $\theta = 160°$ is smaller than that of the rest of the pumping passage. This is perhaps due to the increased rate of flow owing to the internal leakage through the side clearance *c*. The rate of flow near the entry may also be influenced by the internal leakage. However, the pressure gradients near the entry and the exit of Reformed No. 1 type are respectively nearly equal to those of Reformed No. 3 type; that is, the rates of flow are nearly equal in both types of pumps. Accordingly the improvement of the pressure distribution in the reformed pumps is chiefly due to the reformation of the shape of the pumping passage.

If the rate of flow increases, the influence of the entry will result in greater length, thus the length of the enlarged part will not be long enough. Contrarily, if the discharge is less, the length may be too long. It is very difficult and not a good method to find the best length of the enlarged part by the measurement of the pressure distribution in the pumping passage. The purpose of the reformation is to improve the performance of a pump, so the performance should be compared with each other among these reformed pumps and the best shape of the pumping passage should be decided.

7. The performance of the reformed pump. It is out of the question that the pressure decrease near the entry has a large influence on the suction ability of the pump. Additionally, according to the performance equations shown by the present writer, the performance of a pump is influenced by the pressure decrease at the entry. The reformation diminishes the pressure decrease as shown above, so a great improvement is expected in the performance.

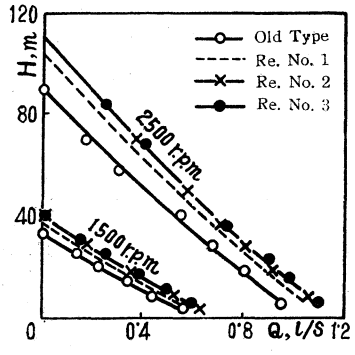

FIG. 4.
Comparison of the head-capacity characteristics of the reformed and the old type pumps.

The relations among the head, the discharge and the speed of revolution are shown in Figure 4. In this figure the performances of the old type, Reformed No. 2 and No. 3 types are the experimental data tested with the existing condition of $c = 0.05$ mm, but the performance of Reformed No. 1 type is the inferred value at $c = 0.05$ mm which is estimated from the experimental data at $c = 0.30$ mm. At every discharge, as this figure shows, the head of Reformed No. 3 type is higher than that of No. 2, No. 2 is higher than No. 1, No. 1 is higher than the old type.

The foregoing report shows that there is the following relation:

$$H=-h+(L-L')\frac{\kappa U}{A\delta g}\left[AU\left\{1+\frac{\varepsilon}{\delta}-\frac{1}{\ln(1+\delta/\varepsilon)}\right\}-Q\right]\Big/\left\{\frac{1}{2}+\frac{\varepsilon}{\delta}-\frac{1}{\ln(1+\delta/\varepsilon)}\right\}.$$

In this equation H is the total head, Q is the discharge, h is the pressure decrease in the pumping passage, L is the structural length of the pumping passage and L' is the ineffective length. The rest of these values are decided by the property of liquid and the shape and the dimension of the pump, which are kept constant in both the old type and reformed types of the pump.

When the discharge is large and the second term of the above equation is small, the total head H is chiefly influenced by the pressure decrease h. That is, when the discharge is large, the difference of the total head among these pumps is nearly equal to the difference of the pressure decrease at

the entry. Accordingly these experimental data shown in Figure 4 illustrate that the pressure decrease diminishes due to the reformation.

Since the pressure decrease h is proportional to square of the discharge, the difference of the pressure decrease becomes less remarkable as the discharge decreases. When the discharge is little, the total head is chiefly influenced by the effective length $(L-L')$, because the second term of the above equation is large. Since L' is proportional to the discharge, L' becomes zero when there is no discharge.

It is clear that the structural length L is longest in the old type pump; Reformed No. 1 is longer than No. 2, which is longer than No. 3. If the other conditions were the same, therefore, the old type pump would produce the highest head among all of these pumps. However, the head is higher at every discharge in this order: Reformed No. 3, No. 2, No. 1 and the old type.

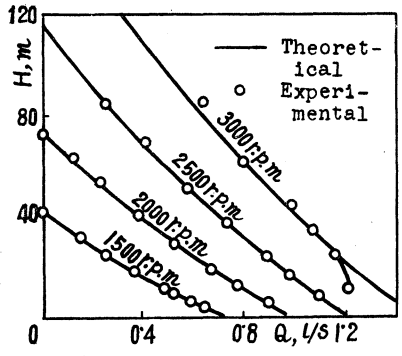

FIG. 5.
Theoretical and experimental head-capacity characteristics of the reformed pump.

Figure 5 shows that the experimental data of Reformed No. 3 type pump perfectly coincide with the inferred performance estimated through the above equation, if only the intensity of turbulence in the pumping passage is assumed properly larger than that of the old type. These experimental data show that the coefficient of turbulence κ is 0.0303 for the old type pump, 0.0333 for Reformed No. 1 type pump, and 0.0365 for Reformed No. 2 and No. 3 type pumps. This means that the turbulence is strengthened by the reformation of the entry.

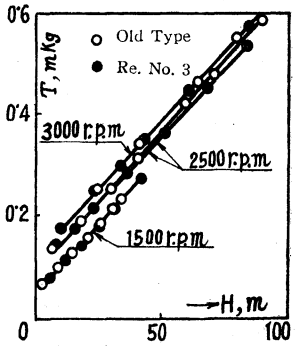

FIG. 6.
Comparison of the torque-head characteristics of the reformed and the old type pumps.

In general, it has been verified[2] both theoretically and experimentally that the turbulent velocity perpendicular to the main flow increases when fluid flows into a narrow passage from a wide passage. If this principle is applicable to the turbulence in the pumping passage of a peripheral pump, the turbulence in the pumping passage of a reformed pump is stronger, because the fluid flows into the pumping passage after the turbulence has developed in the enlarged passage. Contrarily, in the old type pump, the turbulence does not develop before the fluid flows into the pumping passage, but it gradually develops in the narrow pumping passage. Consequently,

[2] Goldstein: Modern development in fluid dynamics. Vol. 1.

the turbulence has not the chance to be strengthened. Since the enlarged range is not long enough in the case of Reformed No. 1 type pump, the turbulence does not adequately develop before the liquid flows into the pumping passage. Therefore, the turbulence is not strong enough even after it is strengthened by flowing into the pumping passage.

According to the foregoing report, there is a linear relation between the torque and the head, and this relation is not influenced by the pressure decrease: i.e. the shape of the entry may be ignored.

$$T = \frac{D}{2} b L \frac{\rho \kappa_0 U^2}{\ln(1+\delta/\varepsilon)} + \frac{D}{4} \rho \delta b \lambda \psi U^2 \left\{1 + \frac{\varepsilon}{\delta} - \frac{1}{\ln(1+\delta/\varepsilon)}\right\}$$
$$+ \frac{D}{2} \rho g b \delta \psi H \left\{1 + \frac{\varepsilon}{\delta} - \frac{1}{\ln(1+\delta/\varepsilon)}\right\}.$$

Figure 6 shows the experimental relationships between the torque and the head of the old type pump and Reformed No. 3 type pump. We can hardly recognize the difference of their relationships. Needless to say, Reformed No. 1 and No. 2 types have just the same relationship as these. That is, these experiments verify the theory that the relationship between the torque and the head is not influenced at all by the pressure decrease at the entry.

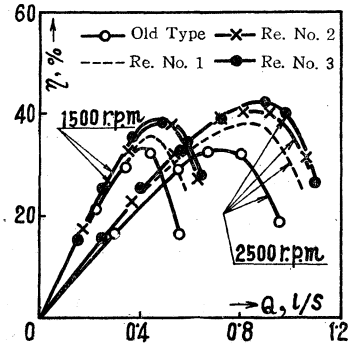

FIG. 7.
Comparison of the efficiencies of the reformed and the old type pumps.

At every head the reformed type pump can discharge more quantity of liquid than the old type pump does in spite of the same torque, accordingly it is quite clear that the efficiency of a pump is improved by the reformation of the entry. Figure 7 shows the comparison of the efficiency among the old type and the reformed type pumps. These experimental data show that the reformation of the entry improves the maximum efficiency by about 9 %. That is, the maximum efficiency of Reformed No. 3 type pump is 1.27 times that of the old type pump.

8. **Performance at cavitation.** Since the reformed entry directly prevents the pressure from decreasing, a remarkable improvement in the suction ability is expected. Figure 8 is a comparison of the performances at suction heads of 4 m and 8 m among the old type pump and three kinds of reformed type pumps. These experimental data show that the maximum discharge at a certain suction head is remarkably influenced by the shape of the entry. As explained in the foregoing paper, these maximum discharges are limited by cavitation induced at the entry of the pumping passage, and the minimum pressure is nearly equal to the vapor pressure of the liquid at that temperature. Accordingly the pressure decrease at the entry is estimated

to be equal to the difference between the suction pressure and the vapor pressure.

As shown in Figure 9, there is a certain relationship between the mean velocity v in the pumping passage and the pressure decrease h' at any speed of revolution. The relationship is approximately shown by the equation $h' = a + k(v^2/2g)$, where a is the pressure decrease due to the centrifugal force or something similar which is not influenced by the rate of flow as well as the speed of revolution. That is, the suction nozzle is connected with the periphery of the pumping passage, while the minimum pressure is induced at the root of the vane of the impeller, so the suction pressure is always higher than the minimum pressure due to the centrifugal force. This pressure difference is not influenced by the shape of the entry and the speed of revolution, keeping 1 m Aq for each of these pumps.

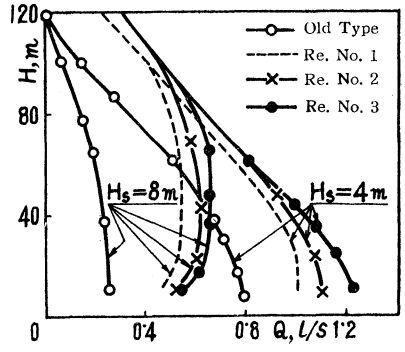

FIG. 8.
Comparison of the suction abilities of the reformed and the old type pumps,

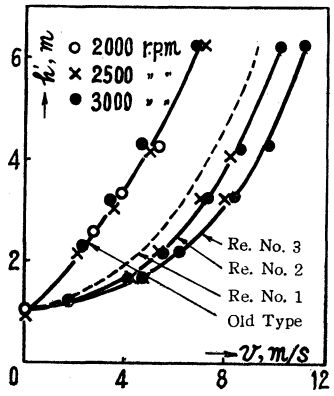

FIG. 9.
Relationships between the pressure decrease and the mean velocity in the pumping passage.

The coefficient of the second term k is a factor which shows the quality of the shape of the entry. Since the value of k of Reformed No. 3 type is 0.65 which is about 1/2.8 of that of the old type, the maximum discharge becomes about $\sqrt{2.8}$ times as much at the same suction head due to this reformation of the entry. The value of k is about $1.5 \sim 1.9$ for most of the pumps already manufactured; that is, it is about the same value as that of the old type pump in this experiment. Therefore, after proper reformation of the entries of conventionall pumps, an improvement of the performance will be expected.

9. Conclusion. The developments of the researches on the influence of the suction port, both theoretical and experimental, are reported together with some results which are of value for the improvement of the pump.

In the first place the cause of the influence of the suction port is studied. By proving that the turbulence is half developed in the pumping passage near the entry, it is found that this is the source of the influence. In order to eliminate this effect, the position of the entry of the pumping passage should be moved down-stream. By doing so, the fluid is disturbed by the

impeller and the turbulence is fully developed before the entry and then the turbulent fluid enters the pumping passage.

The suction port of a pump is reformed into three kinds of forms and the performances of them are compared with each other. The results obtained are:

(1) In order to increase the maximum efficiency of a pump, the entry of the pumping passage should be set in the position of the angular distance of about 65° from the partition.

(2) If the distance between the partition and the entry of the pumping passage is not long enough, sufficient improvement cannot be expected. The value of the maximum efficiency of a pump is largest when there is a certain distance between the partition and the entry, while the suction-ability increases monotonously and asymptotically to a final value when the distance increases.

(3) In the reformed pump the pressure drop at the entry of the pumping passage is not remarkable and cavitation hardly occurs, i.e. the suction-ability of the reformed pump is much larger than that of the old type pump.

(4) The reformed pump discharges more quantity of liquid than the old type pump at both high and low suction-height.

(5) The turbulence in the pumping passage of the reformed pump is more intense and the total head is higher than the old type pump.

(6) In order to deliver a liquid against a total head, the reformed pump need no more input horse-power than the old type pump. Accordingly, the pumping efficiency of the reformed pump increases at the rate of increase of the discharge against the same total head.

(7) The characteristic equations which were induced in regard to the old type pump can be equally applied to the reformed pump, if only the decrease of the pressure drop at the entry and the increase of the intensity of the turbulence are taken into consideration.

The experiments have been conducted under the kind guidance of Professor Kasai, who has helped the writer with useful suggestions. The writer also expresses his deep appreciation for the staff of the Hydraulic Laboratory of Kyushu University who kindly helped the writer in his experiments and for those students who worked with him.

APPENDIX

Assuming that the turbulence in the pumping passage near the entry is not different from that at the rest of the pumping passage, the influence of the entry on the pressure distribution in the pumping passage is calculated. The purpose of this calculation is to clarify whether the strange phenomenon near the entry depends only upon the variation of the velocity profile, so the accurate calculation is not required. Therefore a simple method of analysis is adopted although the accuracy is not so good.

Assuming that the flow is two dimensional, for the sake of simplicity, we take the axis of x along and the axis of y perpendicular to the main flow. Assuming that X, Y are the components of the extraneous force acting on the fluid per unit mass, u, v are the components of the velocity, and u', v' are the components of the turbulent velocity, we can describe the equation of motion as follows:

$$\rho\frac{Du}{Dt}=\rho X-\frac{\partial p}{\partial x}+\frac{\partial}{\partial x}\left(2\mu\frac{\partial u}{\partial x}-\rho\overline{u'u'}\right)+\frac{\partial}{\partial y}\left\{\mu\left(\frac{\partial v}{\partial x}+\frac{\partial u}{\partial y}\right)-\rho\overline{u'v'}\right\}, \quad (1)$$

$$\rho\frac{Dv}{Dt}=\rho Y-\frac{\partial p}{\partial y}+\frac{\partial}{\partial y}\left(2\mu\frac{\partial v}{\partial y}-\rho\overline{v'v'}\right)+\frac{\partial}{\partial x}\left\{\mu\left(\frac{\partial v}{\partial x}+\frac{\partial u}{\partial y}\right)-\rho\overline{u'v'}\right\}, \quad (2)$$

in which ρ is the density and μ is the molecular viscosity. If Reynolds stress is shown by the Businesq's formulae as usual, they are

$$2\mu\frac{\partial u}{\partial x}-\rho\overline{u'u'}=2\mu'\frac{\partial u}{\partial x},$$

$$2\mu\frac{\partial v}{\partial y}-\rho\overline{v'v'}=2\mu'\frac{\partial v}{\partial y},$$

$$\mu\left(\frac{\partial v}{\partial x}+\frac{\partial u}{\partial y}\right)-\rho\overline{u'v'}=\mu'\left(\frac{\partial v}{\partial x}+\frac{\partial u}{\partial y}\right),$$

where μ' is the turbulent viscosity which is a function of location.

The influence of the extranous force or the centrifugal force due to the curvature of the pumping passage is assumed to be very little, it is neglected. Since we assumed that the turbulent viscosity μ' near the entry is equal to that at the rest of the pumping passage, there is a relationship

$$\mu'=\rho\kappa U_0 y \quad (3)$$

where U_0 is the velocity of the moving wall or the peripheral velocity of the impeller, and κ is a coefficient which shows the intensity of the turbulence. Accordingly equations (1), (2) and the equation of continuity are

$$\frac{Du}{Dt}=-\frac{1}{\rho}\frac{\partial p}{\partial x}+2\kappa U_0 y\frac{\partial^2 u}{\partial x^2}+\kappa U_0\left(\frac{\partial v}{\partial x}+\frac{\partial u}{\partial y}\right)+\kappa U_0 y\left(\frac{\partial^2 v}{\partial x\,\partial y}+\frac{\partial^2 u}{\partial y^2}\right), \quad (4)$$

$$\frac{Dv}{\partial t} = -\frac{1}{\rho}\frac{\partial p}{\partial y} + 2\kappa U_0 \frac{\partial v}{\partial y} + 2\kappa U_0 y \frac{\partial^2 v}{\partial y^2} + \kappa U_0 y \left(\frac{\partial^2 v}{\partial x^2} + \frac{\partial^2 u}{\partial x \partial y}\right), \quad (5)$$

$$\partial u/\partial x + \partial v/\partial y = 0. \quad (6)$$

On the surface of the fixed wall $y = \varepsilon$, the turbulent viscosity $\kappa U_0 y$ is equal to the molecular viscosity μ. The depth of the pumping passage is symbolized by h. Assuming that the flow is steady, equation (4) is integrated from $y = \varepsilon$ to $y = \varepsilon + h$ making use of equation (6), thus the following equation is induced:

$$[u\,v]_{\varepsilon}^{\varepsilon+h} - 2\int_{\varepsilon}^{\varepsilon+h} u\frac{\partial v}{\partial y}\,dy = -\frac{h}{\rho}\frac{\partial p}{\partial x} + \kappa U_0 \left\{(h+\varepsilon)\left(\frac{\partial u}{\partial y} - \frac{\partial v}{\partial x}\right)_{\varepsilon+h} - \varepsilon\left(\frac{\partial u}{\partial y} - \frac{\partial v}{\partial x}\right)_{\varepsilon} + 2\int_{\varepsilon}^{\varepsilon+h}\frac{\partial v}{\partial x}\,dy\right\}. \quad (7)$$

The boundary conditions are $\partial v/\partial x = \partial u/\partial x = v = 0$ both on the fixed wall $y = \varepsilon$ and on the moving wall $y = \varepsilon + h$, and $u = 0$ on the fixed wall $y = \varepsilon$. Therefore equation (7) becomes

$$\frac{d}{dx}\int_{\varepsilon}^{\varepsilon+h} u^2\,dy = -\frac{h}{\rho}\frac{dp}{dx} + \kappa U_0 \left\{(\varepsilon+h)\left(\frac{\partial u}{\partial y}\right)_{\varepsilon+h} - \varepsilon\left(\frac{\partial u}{\partial y}\right)_{\varepsilon} - 2\int_{\varepsilon}^{\varepsilon+h}\int_{\varepsilon}^{y}\frac{\partial^2 u}{\partial x^2}\,dy\,dy\right\}. \quad (8)$$

The boundary condition at $y = \varepsilon$ is applied to equation (4), then it is changed into

$$\frac{1}{\rho}\frac{dp}{dx} = \kappa U_0 \left\{\left(\frac{\partial u}{\partial y}\right)_{y=\varepsilon} + \varepsilon\left(\frac{\partial^2 u}{\partial y^2}\right)_{y=\varepsilon}\right\}. \quad (9)$$

In order to exclude the dimensions from the above equations, we adopt new dimensionless symbols θ, ξ, λ and η, where $u = U_0\theta$, $x = h\xi$, $\varepsilon = h\lambda$ and $y = h(\lambda + \eta)$. The following equation is induced from equations (8) and (9):

$$\frac{d}{d\xi}\int_0^1 \theta^2\,d\eta = \kappa\left\{(1+\lambda)\left(\frac{\partial\theta}{\partial\eta}\right)_0^1 - \lambda\left(\frac{\partial^2\theta}{\partial\eta^2}\right)_0 - 2\int_0^1\int_0^{\eta}\frac{\partial^2\theta}{\partial\xi^2}\,d\eta\,d\eta\right\}. \quad (10)$$

In order to solve this equation simply, the velocity profile θ is explained by

$$\theta = \alpha\,\ln\{(\eta+\lambda)/\lambda\} + \beta\eta + \gamma\eta^9 + \delta\eta^{10}. \quad (11)$$

Each of the coefficient α, β, γ and δ in the above equation is a function of ξ. θ must satisfy the following two conditions:

$$[\theta]_{\eta=1} = 1, \quad (12)$$

$$\int_0^1 \theta\,d\eta = K, \quad (13)$$

where K is a dimensionless symbol which shows the rate of flow Q, i.e. $Q = KU_0h$.

The boundary conditions at $\eta = 0$ and $\eta = 1$ are applied to equation (4); it becomes

$$\frac{1}{\rho}\frac{dp}{d\xi} = \kappa U_0^2\left\{\left(\frac{\partial\theta}{\partial\eta}\right)_{\eta=0} + \lambda\left(\frac{\partial^2\theta}{\partial\eta^2}\right)_{\eta=0}\right\} = \kappa U_0^2\left\{\left(\frac{\partial\theta}{\partial\eta}\right)_{\eta=1} + (1+\lambda)\left(\frac{\partial^2\theta}{\partial\eta^2}\right)_{\eta=1}\right\}. \tag{14}$$

Making use of equation (11), equations (12), (13) and (14) are described as follows:

$$\alpha \ln(1+\lambda/\lambda) + \beta + \gamma + \delta = 1,$$
$$\alpha(1+\lambda)\ln(1+\lambda/\lambda) - \alpha + \beta/2 + \gamma/10 + \delta/11 = K,$$
$$\delta = -0.81\gamma.$$

By substituting the value of θ shown in equation (11) for θ in equation (10), an equation will be made which contains α, β, γ, δ, and ξ. By solving this equation together with the three above equations, each of α, β, γ and δ is shown as a function of ξ. An example is shown in the case of $\ln(1+\lambda/\lambda) = 6$. The magnitude of κ in this assumption is about 0.033. Equation (10) becomes

$$\frac{1}{\kappa}\frac{d\gamma}{d\xi}(-0.051 + 0.0435K + 0.0062\gamma) = 0.9\gamma - 0.0284\frac{d^2\gamma}{d\xi^2}.$$

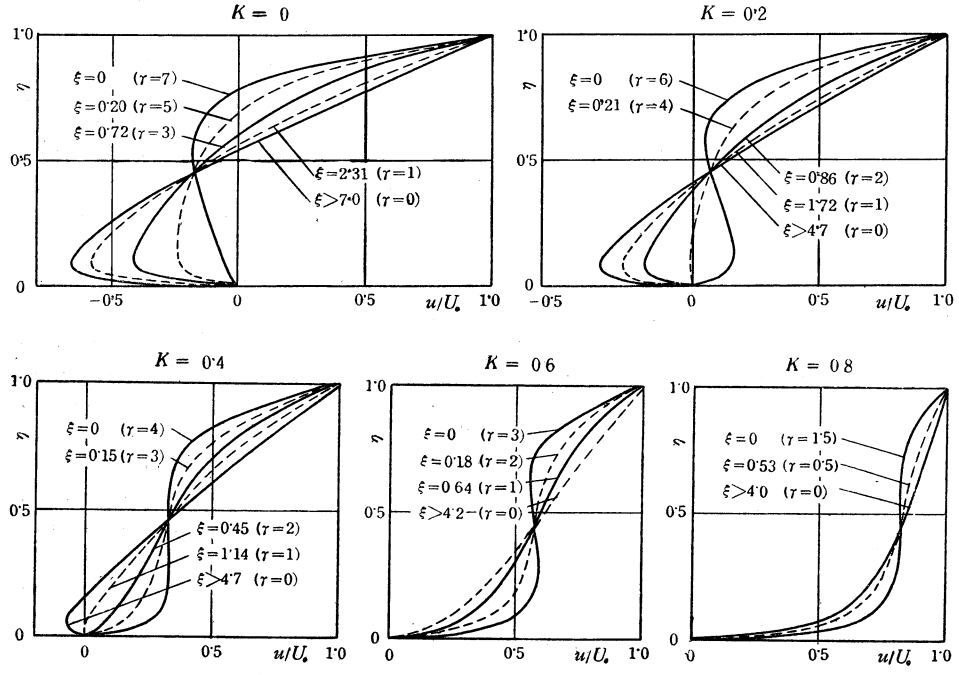

FIG. 10.
Theoretical status of the velocity profile near the entry where the turbulence has developed.

The value of γ at $\xi = 0$ should be decided beforehand. This value γ_0 should be selected so that the velocity in the pumping passage is uniform throughout the cross-section at the entry $\xi = 0$. Such value γ_0 does not remain constant if the rate of flow K varies, but the proper value is easily decided by trials of several times. Additionally, even if the value is not proper, it does not remarkably influence the results of the calculation.

Figure 10 shows some examples of the velocity profiles which are calculated by this method at several cross-sections. As the distance from the entry ξ increases, the value of γ diminishes and tends to zero, which means that there is no influence of the entry at all.

By applying the relation between γ and ξ to equation (14), we can find the relationship between the pressure increase $p/2\rho U_0^2$ and the distance from the entry ξ. This relationship is shown in Figure 11. According to this figure, the pressure gradient near the entry is less than that throughout the rest of the passage, but the difference is not great and the pressure distribution is quite different from that shown in Figure 1. That is, even if the value of the rate of flow K is very large, the range which is influenced by the entry is only about $\xi = 1$. Since the mean depth of the pumping passage h is usually two or three millimeters, the influenced range should then be accordingly in ratio. In the case of $K = 0.8$, the pressure in the pumping passage is lower than that just following the entry point. However, the value is about $0.01 \times U_0^2/2g$, so it is only 0.2 m even in the case of $U_0 = 20$ m/s. Therefore it may be negligible.

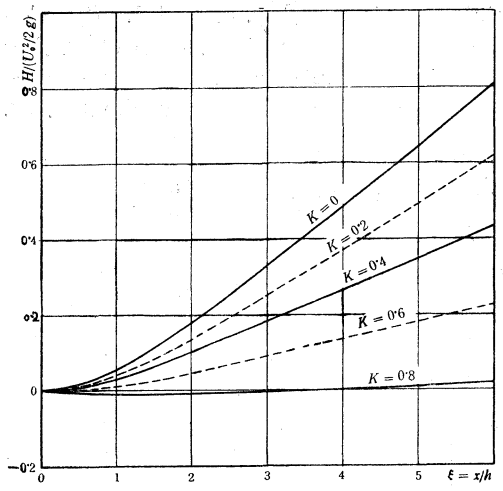

FIG. 11.
Theoretical pressure distributions near the entry where the turbulence has developed.

The results of the calculation mentioned above are quite different from the pressure distributions of peripheral pumps measured experimentally. This means that the turbulence near the entry assumed above is not correct. Since the results of the calculation illustrate that the transition of the velocity profile does not remarkably influence the pressure distribution, we may think that the pressure gradient at each position is nearly proportional to the intensity of the turbulence. Accordingly, the intensity of turbulence near the entry of an actual pump seems to be much weaker than that of the remaining pumping passage.

(Received May 17, 1954)

NOTES

On the Axisymmetric Boundary Value Problems in the Transversely Isotropic Elasticity Theory

By Masakazu HIGUCHI

Using the functions $F_m(r, z_m)$ satisfying the equations[1]

$$\left(\frac{\partial^2}{\partial r^2}+\frac{1}{r}\frac{\partial}{\partial r}+\frac{\partial^2}{\partial {z_m}^2}\right)F_m=0, \quad (m=1,2) \tag{1}$$

with which the four components of stresses are expressed as

$$\left.\begin{aligned}
\sigma_r &= \sum_{m=1}^{2}\left(k_m^2\frac{\partial^2}{\partial r^2}+\frac{l_m^2}{r}\frac{\partial}{\partial r}\right)F_m \equiv \sum_{m=1}^{2}L_{rm}(F_m)\\
\sigma_\theta &= \sum_{m=1}^{2}\left(l_m^2\frac{\partial^2}{\partial r^2}+\frac{k_m^2}{r}\frac{\partial}{\partial r}\right)F_m \equiv \sum_{m=1}^{2}L_{\theta m}(F_m)\\
\sigma_z &= \sum_{m=1}^{2}\frac{\partial^2}{\partial {z_m}^2}F_m \equiv \sum_{m=1}^{2}L_{zm}(F_m)\\
\tau_{rz} &= \sum_{m=1}^{2}k_m\frac{\partial^2}{\partial r\,\partial z_m}F_m \equiv \sum_{m=1}^{2}L_{rzm}(F_m)
\end{aligned}\right\} \tag{2}$$

we can obtain the solutions of boundary value problems of transversely isotropic medium subjected to torsionless axisymmetric tractions on the boundary or to prescribed axisymmetric displacements of the boundary when the boundaries are of such simple form as mentioned in the following.

The stress-strain relations[2] of transversely isotropic medium, the equations of compatibility[3] and the stress equations of equilibrium[4] are, as shown easily, satisfied by the functions $F_m(r, z_m)$, $m=1,2$ together with the expressions (2).

Especially, for an isotropic medium

$$k_m \to 1, \quad l_m \to 0 \quad (m=1,2).$$

---

1)

$$k_1^2+k_2^2=\frac{2\nu_{rz}}{1+\nu_{r\theta}}+\frac{g_{rz}^2}{1-\nu_{r\theta}^2}$$
$$k_1^2k_2^2=\frac{e_{rz}^2-\nu_{rz}^2}{1-\nu_{rz}^2}$$
$$l_m^2=\nu_{rz}-\nu_{r\theta}k_m^2$$
$$z_m=k_m z \quad (m=1,2)$$
$$e_{rz}^2=E_{rr}/E_{zz}, \quad g_{rz}^2=E_{rr}/G_{rz}$$
$$\nu_{r\theta}=E_{rr}/E_{r\theta}, \quad \nu_{rz}=E_{rr}/E_{rz}.$$

2)

$$\varepsilon_r=\frac{\partial u}{\partial r}=\frac{\sigma_r}{E_{rr}}+\frac{\sigma_\theta}{E_{r\theta}}+\frac{\sigma_z}{E_{rz}}$$
$$\varepsilon_\theta=\frac{u}{r}=\frac{\sigma_r}{E_{\theta r}}+\frac{\sigma_\theta}{E_{\theta\theta}}+\frac{\sigma_z}{E_{\theta z}}$$
$$\varepsilon_z=\frac{\partial w}{\partial z}=\frac{\sigma_r}{E_{zr}}+\frac{\sigma_\theta}{E_{z\theta}}+\frac{\sigma_z}{E_{zz}}$$
$$\gamma_{rz}=\frac{\partial u}{\partial z}+\frac{\partial w}{\partial r}=\frac{\tau_{rz}}{G_{rz}}.$$

3)

$$\frac{\partial^2\varepsilon_r}{\partial z^2}+\frac{\partial^2\varepsilon_z}{\partial r^2}=\frac{\partial^2\gamma_{rz}}{\partial r\,\partial z}$$
$$\frac{\partial}{\partial r}(r\varepsilon_\theta)-\varepsilon_r=0.$$

4)

$$\frac{\partial\sigma_r}{\partial r}+\frac{\partial\tau_{rz}}{\partial z}+\frac{\sigma_r-\sigma_\theta}{r}=0$$
$$\frac{\partial\tau_{rz}}{\partial r}+\frac{\partial\sigma_z}{\partial z}+\frac{\tau_{rz}}{r}=0.$$

The expressions of stress components then degenerate into

$$(\sigma_\theta)_{iso} = \frac{-1}{r}\frac{\partial}{\partial r}(F_u - 2F_2) + 2\nu\frac{\partial^2}{\partial r^2}F_2, \quad (\sigma_r)_{iso} = -\frac{\partial^2}{\partial r^2}(F_u - 2F_2) + \frac{2\nu}{r}\frac{\partial}{\partial r}F_2$$

$$(\sigma_z)_{iso} = \left(\frac{\partial^2}{\partial r^2} + \frac{1}{r}\frac{\partial}{\partial r}\right)F_u$$

$$(\tau_{rz})_{iso} = -\frac{\partial^2}{\partial r\,\partial z}F_u,$$

where F_u is the same function as given by C. Weber and

$$F_u \equiv -F_1 - z\frac{\partial F_2}{\partial z}$$

is the relation with our functions.

Denoting the tractions on the boundary S in the directions of the axis r and z with $p_r\,dS$ and $p_z\,dS$ respectively, we obtain the expressions

$$\left.\begin{aligned} p_z &= \left\{-\sigma_z\frac{dr}{dS} + \tau_{rz}\frac{dz}{dS}\right\}_S = \sum_{m=1}^{2}\left\{\frac{1}{r}\frac{d}{dS}\left\{r\frac{\partial F_m}{\partial r}\right)\right\}_S \\ p_r &= \left\{\sigma_r\frac{dz}{dS} - \tau_{rz}\frac{dr}{dS}\right\}_S = \sum_{m=1}^{2}\left\{\frac{l_m^2 - k_m^2}{r}\frac{\partial F_m}{\partial r}\frac{dz}{dS} - \frac{d}{dS}\left(\frac{\partial F_m}{\partial z}\right)\right\}_S. \end{aligned}\right\} \quad (3)$$

On the other hand, the displacements $\{u\}_S$ and $\{w\}_S$ on the boundary in the directions of the axes r and z are expressed as

$$\left.\begin{aligned} \frac{E_{zr}}{1-\nu_{r\theta}}\{u\}_S &= \sum_{m=1}^{2}\left\{\left(\frac{1+\nu_{r\theta}}{\nu_{rz}}k_m^2 - 1\right)\frac{\partial F_m}{\partial r}\right\}_S \\ \frac{E_{zr}}{1-\nu_{r\theta}}\{w\}_S &= \sum_{m=1}^{2}\left\{\left(\frac{e_{rz}^2 - \nu_{rz}^2}{[1-\nu_{r\theta}]\,\nu_{rz}\,k_m^2} - 1\right)\frac{\partial F_m}{\partial z}\right\}_S \end{aligned}\right\} \quad (4)$$

respectively.

The convenient forms of the solution F_m in either case of the first and the second kind of conditions given on the boundary are selected from

$$F_m(r, z_m) = \int_C f_m(\alpha)\,e^{\alpha z_m}\,C_0(\alpha r)\,d\alpha, \quad (z_m = k_m z) \qquad (5)$$

$$F_m(r_m, z) = \int_C f_m(\alpha)\,e^{\alpha z}\,C_0(\alpha r_m)\,d\alpha, \quad (r_m = r/k_m) \qquad (6)$$

where $f_m(\alpha)$ = functions to be determined to satisfy the boundary conditions and

$C_0(\alpha r)$, $C_0(\alpha r_m)$ = cylindrical functions of the O-th order.

The integration with respect to α is done along a curve C chosen appropriately for each case.

Thus, to solve the obtained integral equation is merely to transform the equation by use of the Hankel's relation of the cylindrical functions and to solve the derived algebraic simultaneous equations with respect to $\overline{f_m(\alpha)}$, $f_m(\alpha)$, $(m = 1, 2)$.

For instances,

$$F_m(r, z_m) = \int_0^\infty f_m(\alpha)\,e^{\alpha z_m}\,J_0(\alpha r)\,d\alpha, \quad (z_m = k_m z) \qquad (7)$$

is the function for the semi-infinite body with the boundary

$$\{z\}_S \equiv \zeta = 0 .$$

The solutions are

$$F_m(r, z_m) = \int_0^\infty \frac{\Delta_m(\alpha)}{\Delta} e^{\alpha z_m} J_0(\alpha r)\, d\alpha \qquad (m = 1, 2), \tag{8}$$

where

$$\Delta = k_2 - k_1$$

$$\Delta_m(\alpha) = (-1)^m \begin{vmatrix} 1 & A(\alpha) \\ k_n & B(\alpha) \end{vmatrix} \qquad \begin{pmatrix} m, n = 1, 2 \\ m \neq n \end{pmatrix}$$

$$A(\alpha) = -\frac{1}{\alpha} \int_0^\infty p_z(\rho)\, J_0(\alpha \rho)\, \rho\, d\rho$$

$$B(\alpha) = \frac{1}{\alpha} \int_0^\infty p_r(\rho)\, J_1(\alpha \rho)\, \rho\, d\rho$$

for the case of the lst-kind and

$$\Delta = \begin{vmatrix} a_1 & a_2 \\ k_1 b_1 & k_2 b_2 \end{vmatrix}$$

$$\Delta_m(\alpha) = (-1)^m \begin{vmatrix} a_n & A(\alpha) \\ k_n b_n & B(\alpha) \end{vmatrix} \qquad \begin{pmatrix} m, n = 1, 2 \\ m \neq n \end{pmatrix}$$

$$a_m = \frac{1 + \nu_{r\theta}}{\nu_{rz}} k_m^2 - 1$$

$$b_m = \frac{e_{rz}^2 - \nu_{rz}^2}{[1 - \nu_{r\theta}]\, \nu_{rz}\, k_m^2} - 1$$

$$A(\alpha) = -\frac{E_{rz}}{1 - \nu_{r\theta}} \int_0^\infty u(\rho)\, J_1(\alpha \rho)\, \rho\, d\rho$$

$$B(\alpha) = \frac{E_{zr}}{1 - \nu_{r\theta}} \int_0^\infty w(\rho)\, J_0(\alpha \rho)\, \rho\, d\rho$$

for the case of the 2nd-kind. Stresses are calculated by the formulae[5]

$$\sigma_\mu = \sum_m \int_0^\infty \frac{\Delta_m(\alpha)}{\Delta} L_\mu \{e^{\alpha z_m} J_0(\alpha r)\}\, d\alpha \qquad (\mu = r, \theta, z, rz) .$$

Similarly the problems can be solved for the following bodies;

(a) infinite plate perpendicular to the axis z,
(b) infinite solid circular cylinder parallel to the axis z,
(c) infinite body having a circular cylindrical hole with its axis parallel to the axis z, and
(d) infinite hollow circular cylinder with finite thickness and with its axis parallel to the axis z.

(Received April 30, 1954)

[5] As to the formulae for quasi-isotropic medium and for other examples mentioned below, see the Japan Soc. Mech. Engr., Trans., Vol. 15, No. 50, Part 1, p. 100 (1949) and do. Vol. 16, No. 55, p. 67 (1950).